

PAPER • OPEN ACCESS

A Discrete Element Framework for the modelling of rock-filled gabions

To cite this article: Nicola Marigo *et al* 2021 *IOP Conf. Ser.: Earth Environ. Sci.* **833** 012102

View the [article online](#) for updates and enhancements.

A promotional banner for the 240th ECS Meeting. The banner features a colorful striped border at the top. On the left, the ECS logo is displayed in a green circle. To its right, the text reads: "240th ECS Meeting", "Digital Meeting, Oct 10-14, 2021", "We are going fully digital!", "Attendees register for free!", and "REGISTER NOW" in bold orange letters. On the right side of the banner, there is a photograph of a diverse group of people in a professional setting, with a man in a white shirt and tie clapping and smiling.

ECS **240th ECS Meeting**
Digital Meeting, Oct 10-14, 2021
We are going fully digital!
Attendees register for free!
REGISTER NOW

A Discrete Element Framework for the modelling of rock-filled gabions

Nicola Marigo¹, Fabio Gabrieli¹, Antonio Pol¹, Alberto Bisson²,
Lorenzo Brezzi¹

¹ University of Padova, dept. of Civil, Environmental and Architectural Engineering, via
Ognissanti 39, Padova, Italy

² Sirive s.r.l., via A. Fogazzaro 71, Cornedo Vicentino, Vicenza, Italy

E-mail: fabio.gabrieli@unipd.it

Abstract. Gabions are steel mesh cages filled with stones. Recently, they have had a great diffusion for numerous applications such as erosion control and soil retention along cuts and natural slopes. The study of their mechanical behaviour under different loading conditions is a fundamental prerequisite for an improved understanding of their overall performance and in a design perspective. In this respect, the Discrete Element Method (DEM) appears a robust and effective technique. The DEM is particularly suited for modelling granular materials, and recently it has efficiently been applied for modelling deformable structures such as welded meshes. This work presents a discrete framework for the modelling of rock-filled gabions. The gabion module is modelled as an assembly of deformable cylindrical elements, while the filling material is represented using rigid aggregates of spherical particles. The tensile behaviour of the gabion elements is set in order to fit the mechanical response of the steel bars adopted in practice. The model is applied to analyse a uniaxial compression test on a single gabion.

1. Introduction

Gabions are cellular structures fabricated from a steel mesh and filled with rocks. These elements are nowadays largely applied in engineering practice. They are considered to be a “green” structural solution and their applications range from retaining structures to riverbank erosion control (see Figure 1a).

Gabion cells are characterised by a non-trivial mechanical behaviour. On one hand, the structural cage permits the self-stability of the cell and provide confinement of the filling material; on the other hand, the latter provides an internal resistance that permits the gabion cell to support significant external loads. Finally, the discrete nature of the granular filling determines that its interaction with the structural elements and local effects (e.g. force localisation due to stones alignment) may largely affect the overall behaviour of the gabion.

In this work, the discrete element method (DEM) is adopted in order to simulate a rock-filled welded gabion unit. A particle-based approach is in fact well suited to deal with coarse granular materials such as the gabion filling material. Moreover, the effectiveness of a discrete element approach for simulating wire mesh cellular or flexible retaining structures has already been proven [1–13]. The recent introduction of deformable cylindrical elements [14, 15] has open the possibility of analysing beam-like elements in a discrete element framework.



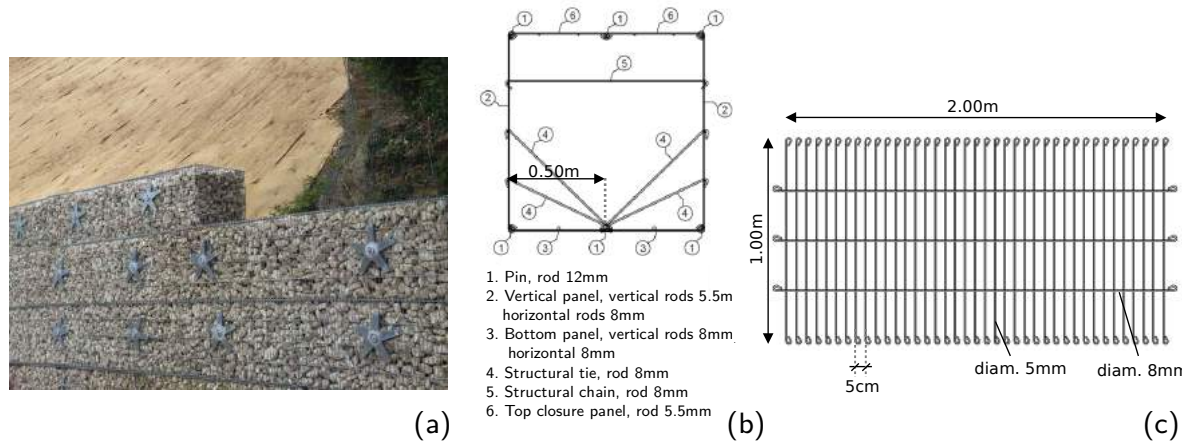


Figure 1. (a) Tie-back earth structure made of gabions combined with self-drilling anchors. (b) Transversal section showing the internal bracing system and (c) frontal view of the gabion's panel.

In the present study, the welded gabion module produced by Sirive s.r.l. company is considered. The geometry of the gabion and the layout of its components are shown in Figure 1b-c. This work aims to propose an approach for the modelling of welded gabions.

The paper is organised as follows. Firstly, the numerical approach and the model of the gabion module are described (Sec. 2). Secondly, a compression test on the gabion steel cage is presented (Sec. 3). Finally, a compression test on the filled gabion module is reported (Sec. 4). The numerical simulations presented in this work are performed with the open-source code YADE [16].

2. Numerical methodology

2.1. Gabion structural elements

The structural elements of the gabion cage (i.e. steel bars) are described as a collection of interconnected cylindrical elements. A cylindrical element (see Figure 2a) is geometrically defined as the Minkowski sum of a sphere and a segment; it behaves like a standard discrete element, but it may deform along its longitudinal direction according to the relative displacement of the extremities nodes. The interaction between the cylinder's nodes is ruled by a user-defined contact law. This permits one to model elastic perfectly plastic beams which are able to withstand normal, shearing, bending and twisting loadings. Further details about the implementation of cylindrical elements can be found in [14, 15].

In this work, cylindrical elements of length 2.5cm are used to discretise the structure of the gabion; therefore, the 1m and 2m length steel bars are subdivided into 40 and 80 cylindrical elements respectively. This discretisation permits a smooth representation of the geometry of the bars elements and the behaviour of the latter to be correctly represented also at large displacements [14].

The gabion module here considered is composed of three different steel bar types characterised by a diameter of 5.5mm, 8mm and 12mm respectively (see Figure 1b-c). The bars composing the internal bracing systems have a diameter of 8mm; differently from the bars belonging to the external cage, the elements of the bracing system are modelled as a single cylindrical element since they are supposed to mainly experience tensile loading in serviceability conditions. The tensile behaviour of the cylinder elements (i.e. the interaction between nodal particles) is perfectly elastic with an ultimate tensile strength of 500MPa and an elastic modulus of 210GPa.

Micromechanical elastic modulus, E_m^c	2.1e11 Pa
Tangent to normal contact stiffness coefficient, ν_m^c	0.3
Contact friction angle, ϕ_m^c	30°

Table 1. Numerical parameters of the cylinder elements.

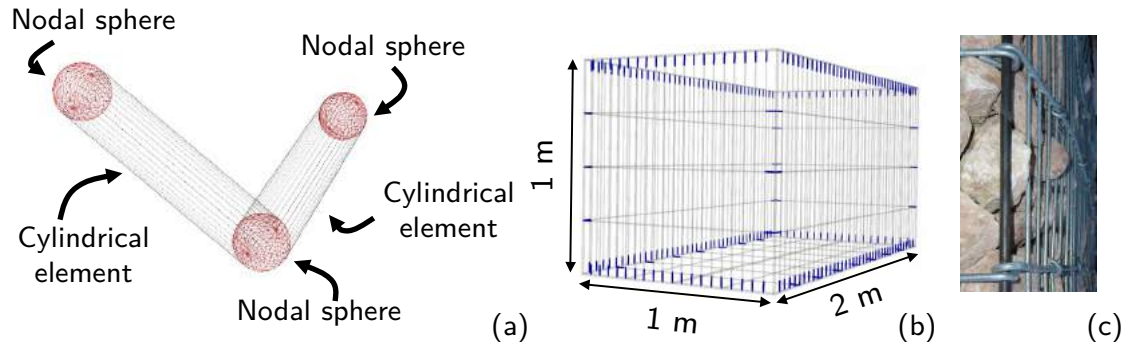


Figure 2. (a) Graphical scheme of two interconnected cylindrical elements. (b) 3D view of the model of the gabion cage (elements schematising the hooked end of the bars are highlighted in blue). (c) View of the hooked ends of the gabion's bars.

The capability of the model of accounting for buckling of the bars is verified by performing ad-hoc simulations (the three bar's diameters are considered) in which a 1m length bar is axially loaded. All the degrees of freedom of the bottom extremity node are fixed, while the top extremity node can translate only along the bar axis. A very slight asymmetry of the bar is imposed by laterally shifting the position of the top extremity node by 0.1mm from the bar's longitudinal axis. The compressive load is applied by a moving plate (displacement rate of 0.5mm/s) in contact with the top node of the bar. The buckling load numerically obtained (i.e. maximum force before the bar instability) are compared with Euler critical load theory. A difference lower than 6% is observed from the analytical solution confirming that the model is able to account for the onset of buckling.

The numerical model of the gabion module is shown in Figure 2b. The gabion side panels are joined together by inserting the 12mm bars in the hooked end of the 5.5mm and 8mm bars (see Figure 2c). In the numerical model, the real geometry of the hooked ends is replaced with cylindrical elements (blue elements in Figure 2b) whose maximum tensile resistance correspond to the opening load of the hooks (i.e. 5kN). The contact parameters of the cylindrical elements are summarised in Table 1.

2.2. Filling material

The filling material plays a key role in the behaviour of the gabion module. In fact, it permits the cellular structure to sustain high compressive and shear loads, as well as the transmission of static and dynamics loads coming from anchor plates or impacting objects. Different granular materials can be used as filling material ranging from rounded pebbles to very angular quarry stones depending on the gabion module and on the available materials on site. The geometrical and mechanical characteristics of the filling material will affect the module resistance. Moreover, the filling procedure may strongly influence the final mechanical behaviour of the module having this a direct impact on the degree of compaction of the granular filling.

Micromechanical elastic modulus, E_m^s	2.85e8 Pa
Tangent to normal contact stiffness coefficient, ν_m^s	0.3
Contact friction angle, ϕ_m^s	70°

Table 2. Numerical parameters of the filling material.

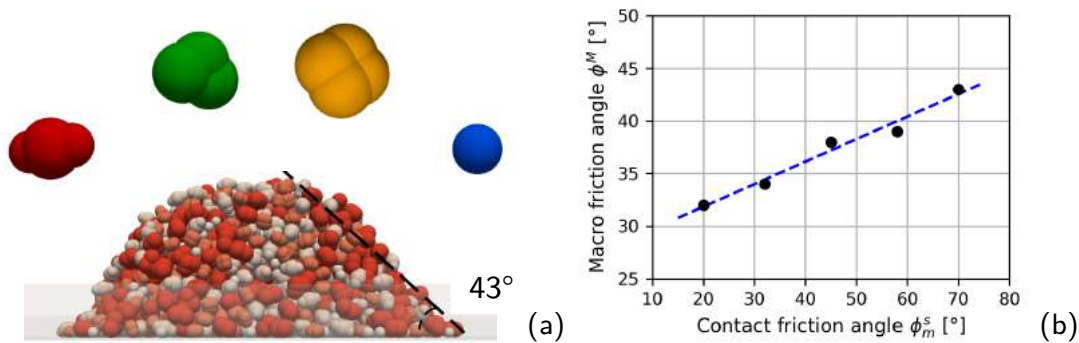


Figure 3. (a) View of the filling material at the end of the heap test and of different clumps shapes. (b) Repose angle of the granular pile ϕ^M as a function of the contact friction angle ϕ_m^s .

In this work, rigid aggregates of spherical particles (i.e. clumps) are adopted for the numerical description of the filling material. Four clump types are used, whose geometry is shown in Figure 3a. The choice of the dimensions of the clumps has been made according to the guidelines of the manufacturer: the minimum axis should be greater than 1.5 times the mesh opening size.

The contact friction angle has been calibrated in order to fit the range of the macroscopic friction angle recommended by the manufacturer ($40^\circ \leq \phi^M \leq 45^\circ$). The other contact parameters are reasonably assumed according to values reported in the literature for similar applications [5, 17]. In this perspective, a cloud of particles is let settle under gravity on a plane. The angle of the thus obtained granular pile is measured, once the sample has reached a stable configuration. A view of the granular sample at the end of the heap test is reported in Figure 3a for the sake of clarity.

The influence of the contact friction angle on the macroscopic friction angle granular material is shown in Figure 3b. The contact parameters of the filling material are reported in Table 2.

3. The behaviour of the gabion cage under compression

The mechanical behaviour of the gabion steel cage is here investigated in unconfined compression conditions. In the test setup the bottom panel of the cage is fixed (i.e. all the degrees of freedom of the bottom panel's nodal particles are fixed), while the top border (i.e. the part in contact with the plate) can translate only along the vertical direction. The compressive load is applied through a flat plate, which is moved downwards at a fixed displacement rate of 1cm/s (see Figure 4a). During the test, the force acting on the plate as well as the displacement of the latter are registered, thus providing as output a force-displacement relation as reported in Figure 4b. The test is considered finished after a displacement of the plate of 5cm.

Observing the trend of the force-displacement curve reported in Figure 4b it can be noted that the gabion cage initially provides a strong contrast to the plate displacement; subsequently, the vertical bars suddenly buckle determining a step-wise force-displacement response with a gradual loss of the gabion compressive resistance. The instability of the vertical bars is evident

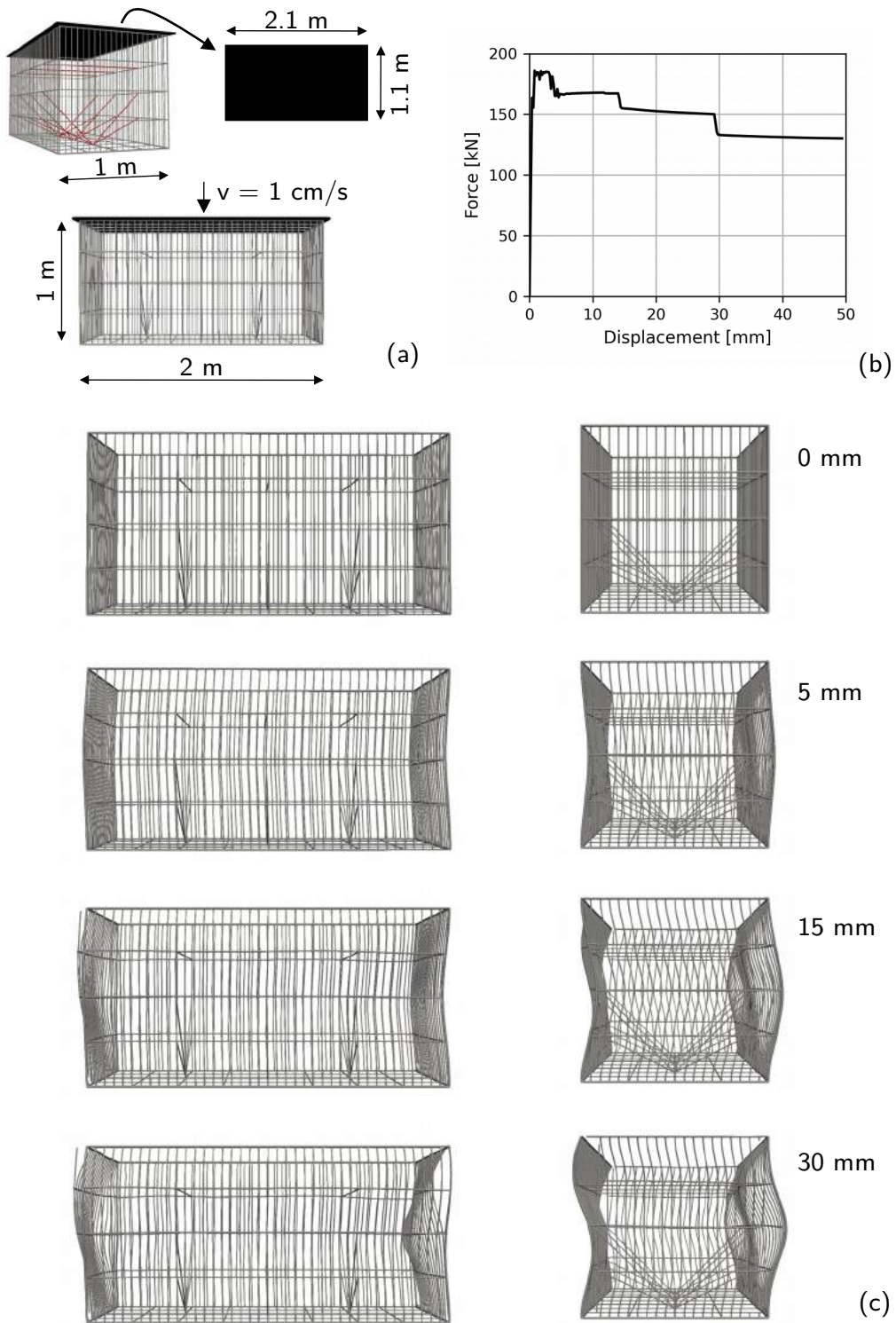


Figure 4. (a) 3D view of the compression test geometry. (b) Force-displacement curve. (c) Lateral views of the gaban cage at different steps of the compression test.

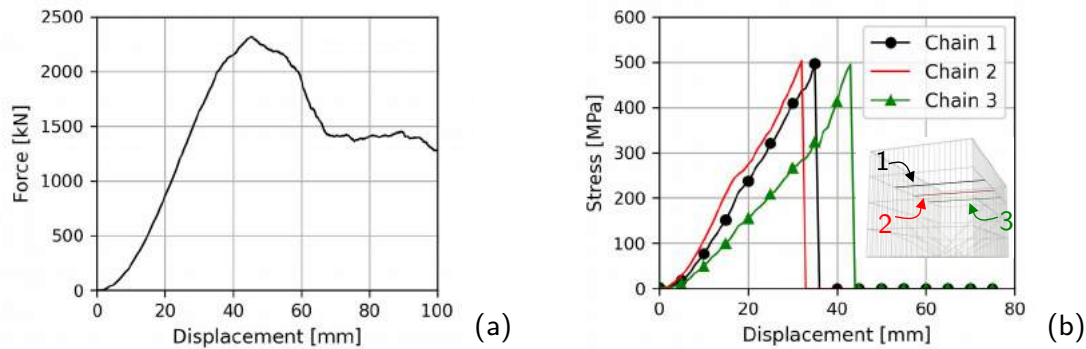


Figure 5. (a) Force-displacement curve. (b) Tensile stress acting on the chains of the bracing system as a function of the plate displacement.

observing the lateral views of the gabion cage during the test reported in Figure 4c.

4. The behaviour of the filled gabion module under compression

After having tested the solely steel cage, the mechanical behaviour of the filled gabion module is addressed. A similar test setup to the one presented in Sec. 3 is adopted, but in this case the gabion is filled with the granular material described in Sec. 2.2. Furthermore, the dimension of the loading plate is slightly reduced (i.e. $0.9\text{m} \times 1.9\text{m}$) in order to impose the load directly on the filling material. This permits a better contact between the moving plate and the filling material to be obtained.

Before the beginning of the compression test, the gabion module is filled through a two-phase procedure. Firstly, a cloud of particles is let settle inside the gabion under gravity. Secondly, a temporary external force, in the normal directions to the gravity force, is iteratively applied to the particles aiming to mimic a vibratory compaction until reaching the desired porosity (i.e. $n=0.29$). This phase permits a higher compaction of the granular filling to be reached. Finally, the particles that are outside the gabion cage are removed and the top surface of the granular volume is regularised. After this preliminary phase, the displacement rate (1cm/s) is imposed to the loading plate, thus stating the test; the latter is ended after a displacement of the plate equal to 10cm for which most of the bracing elements have failed and severe ruptures in the gabion cage (e.g. detachment of the panels at the cage's corners) are observed. During the test, the force acting on the plate as well as the displacement of the latter are registered, thus providing as output a force-displacement relation. From the force-displacement curve reported in Figure 5a, it can be observed that after the initial regularisation of the contact surface between the plate and the filling material (i.e. plate displacement $<5\text{ mm}$) there is a linear increment of the force with the plate displacement. Subsequently, for a displacement greater than approximately 35mm a change in the trend of the force-displacement curve is observed; this is caused by both the breakage of some of the cylinders connecting the gabion's panels and the progressive failure of the elements of the bracing system. In particular, the failure of the upper internal horizontal chains determines an increase of the lateral deformability of the gabion module and consequently a sudden reduction of the soil confinement under the plate. Once the internal chains have failed, a strong drop of the force-displacement curve is observed (i.e. plate displacement $>45\text{ mm}$) and the progressive failure of the connections between the gabion panels is observed. In the last part of the test (i.e. plate displacement $>70\text{ mm}$), the force seems to stabilise to a constant value showing that, even if the gabion cage has undergone several ruptures it is still able to apply a "residual" confining action on the filling material. At the end of the test, the gabion is

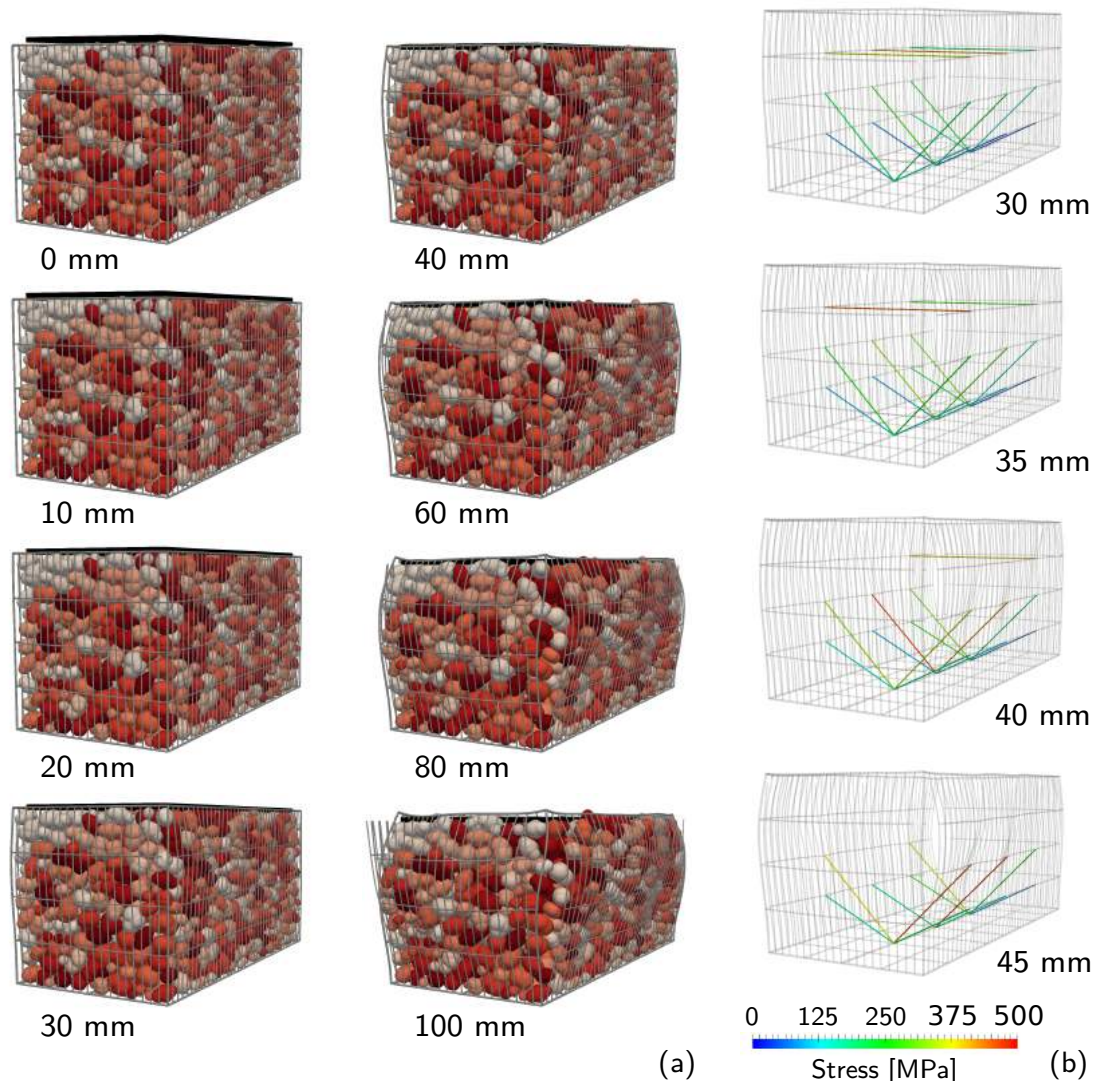


Figure 6. (a) 3D views of the gabion module and (b) tensile stress acting on the internal bracing system at different steps of the compression test.

significantly deformed and shows severe ruptures along its edges. The progressive deformation of the gabion module during the compression test can be appreciated from the 3D views of the model reported in Figure 6a.

The adopted modelling approach permits one to access the mechanical condition of each cylinder elements during the simulation. For instance, the evolution of the tensile stress in the chains of the internal bracing system as a function of the plate displacement is reported in Figure 5b. Firstly, it can be noted that, as expected, the central chain (chain 2) shows a prompt response in contrasting the plate displacement; the central chain is also the first element of the bracing system to break as shown in Figure 6b. Secondly, it is interesting to note that, even if the chains 1 and 3 are placed symmetrically with respect to the middle section of the gabion module, they contribute at a different time to the gabion mechanical response. For the same level of the plate displacement, the contribution of the chain 1 is higher than the one provided by the chain 3; this may be related to a non-homogeneous redistribution of the load in the filling material due to local effects deriving from geometrical irregularities in the granular

packing. This result shows that, differently from a continuum-based approach, the adoption of a particle-based approach allows local effects to be accounted for. The progressive breakage of the elements of the bracing system can be observed in Figure 6b.

5. Conclusions

In this work, an approach based on the discrete element method for the analysis of the mechanical behaviour of welded gabion modules has been presented. This approach combines the effectiveness of the DEM in simulating granular materials to the possibility of modelling grid-like deformable structures introduced by the recent development of deformable cylindrical elements. Despite the simplifications on the particles' shape and the steel bar mechanical behaviour, this work had put the light on the potential of the presented approach for investigating rock-filled cellular structures. In the authors' perspective, the peculiar capability of the DEM in handling local effects and ruptures of the gabion's elements is of significant importance for a realistic description of the behaviour of gabion structures.

The compression tests described in the present work represent a preliminary step in the definition of a numerical framework for the modelling of rock-filled gabion modules. It should be noted that the force-displacement relations here presented have to be seen as a qualitative description of the mechanical response of the gabion module, since a calibration of the model with real-scale tests is still undergoing. The effect of using more complex particles' shapes and the adoption of breakable aggregates of particles are currently under investigation.

6. Acknowledgements

The authors would like to acknowledge Sirive s.r.l. for providing data and materials.

References

- [1] Bertrand D, Nicot F, Gotteland P and Lambert S 2005 *Comp Geotech* **32** 564–577
- [2] Nicot F, Gotteland P, Bertrand D and Lambert S 2007 *International Journal for Numerical and Analytical Methods in Geomechanics* **31** 1477–1515
- [3] Thoeni K, Lambert C, Giacomini A and Sloan S W 2013 *Comp Geotech* **49** 158–169
- [4] Thoeni K, Giacomini A, Lambert C, Sloan S W and Carter J P 2014 *International Journal of Rock Mechanics and Mining Sciences* **68** 107–119 ISSN 1365-1609
- [5] Effeindzourou A, Thoeni K, Giacomini A and Wendeler C 2017 *Comput Geotech* **87** 99–114
- [6] Albaba A, Lambert S, Kneib F, Chareyre B and Nicot F 2017 *Rock Mech. Rock Eng.* **50** 3029–3048
- [7] Gabrieli F, Pol A and Thoeni K 2017 Comparison of two DEM strategies for modelling cortical meshes. *Proc. Particle-based Methods - Fundamentals and Applications* pp 489–496
- [8] Gabrieli F, Pol A, Thoeni K and Mazzon N 2018 Particle-based modelling of cortical meshes for soil retaining applications *Numerical Methods in Geotechnical Engineering IX. London: CRC Press* pp 391–397
- [9] Pol A, Gabrieli F, Thoeni K and Mazzon N 2018 Discrete element modelling of a soil-mesh interaction problem *Geomechanics and Geodynamics of Rock Masses* (CRC Press/Balkema) pp 877–882
- [10] Pol A, Gabrieli F and Mazzon N 2020 Enhancement of Design Methodologies of Anchored Mesh Systems Using the Discrete Element Method *Geotechnical Research for Land Protection and Development* (Springer International Publishing) pp 500–508
- [11] Pol A, Gabrieli F and Brezzi L 2021 *Acta Geotech*
- [12] Pol A and Gabrieli F 2021 *Comp Geotech* **134**
- [13] Karampinos E and Hadjigeorgiou J 2021 *Geotech. Geol. Eng.* **39** 359–376
- [14] Bourrier F, Kneib F, Chareyre B and Fourcaud T 2013 *Ecol Eng* **61** 646–657
- [15] Effeindzourou A, Chareyre B, Thoeni K, Giacomini A and Kneib F 2016 *Geotext Geomembr* **44** 143–156
- [16] Šmilauer V *et al.* 2015 Reference manual *Yade Documentation 2nd ed* (The Yade Project) <http://yade-dem.org/doc/>
- [17] Lorentz J 2007 *Etude de la capacité de dissipation sous impact d'une structure sandwich de protection contre les chutes de blocs rocheux* Ph.D. thesis Université Joseph-Fourier - Grenoble I